

南秦岭迷魂阵岩体 LA-ICP-MS 锆石 U-Pb 年代学和 Lu-Hf 同位素特征*

阎明 刘树文** 李秋根 杨朋涛 王伟 郭荣荣 白翔 邓正宾

YAN Ming, LIU ShuWen**, LI QiuGen, YANG PengTao, WANG Wei, GUO RongRong, BAI Xiang and Deng ZhengBin

北京大学地球与空间科学学院,造山带与地壳演化教育部重点实验室,北京 100871

Key Laboratory of Orogenic Belt and Crustal Evolution, Ministry of Education, School of Earth and Space Sciences, Peking University, Beijing 100871, China

2013-05-01 收稿, 2013-08-17 改回.

Yan M, Liu SW, Li QG, Yang PT, Wang W, Guo RR, Bai X and Deng ZB. 2014. LA-ICP-MS zircon U-Pb chronology and Lu-Hf isotopic features of the Mihunzhen pluton in the South Qinling tectonic belt. *Acta Petrologica Sinica*, 30(2):390-400

Abstract Mihunzhen pluton, located in Jiangjiagou-Mogouxia-Xiaoling area of Shaanxi Province, emplaced into an older block within the eastern segment of South Qinling tectonic zone. This pluton consists chiefly of diorites, quartz diorites and granodiorites. Field geological relationships and LA-ICP-MS zircon U-Pb isotopic dating results indicate two magmatic emplacement stages of the pluton, namely, diorites at early stage with an age of 885 ± 4 Ma, and quartz diorites-granodiorites at late stage with an age of $\sim 737 \pm 4$ Ma. In situ Lu-Hf isotopic analyses for the dated zircon reveal that the early dioritic magma was mainly derived from partial melting of the depleted mantle, and the late quartz dioritic-granodioritic magmas were from crystallization fractionation of the early dioritic magma, which suffered either contaminations of crustal materials or mixing with a crust-sourced magma.

Key words Zircon U-Pb chronology; Lu-Hf isotopes; Petrogenesis; Mihunzhen pluton; South Qinling tectonic belt

摘要 位于陕西省的姜家沟-磨沟峡-小岭镇地区的迷魂阵岩体,为南秦岭构造带中一个古老地块内的深成侵入体。该岩体主要由闪长岩、石英闪长岩和花岗闪长岩组成。根据野外地质关系和 LA-ICPMS 锆石 U-Pb 定年结果,可将迷魂阵岩体的岩浆作用分为两个阶段:早期岩浆作用阶段主要形成闪长岩,其侵位时代为 885 ± 4 Ma;晚期岩浆阶段主要形成石英闪长岩-花岗闪长岩,其侵位时代为 $\sim 737 \pm 4$ Ma。定年锆石原位 Lu-Hf 同位素分析揭示早期闪长质岩浆主要形成于亏损地幔的部分熔融,晚期石英闪长岩-花岗闪长岩岩浆主要来源于早期闪长质岩浆的结晶分异,并经历了地壳物质的混染或者壳幔岩浆混合作用。

关键词 锆石 U-Pb 年代学;Lu-Hf 同位素;岩石成因;迷魂阵岩体;南秦岭构造带

中图法分类号 P588.122; P597.3

横亘中国中部的秦岭造山带是连接华北克拉通和华南克拉通的主要造山带(张国伟等,2001),向东与大别-苏鲁超高压变质带相连,其西与祁连-昆仑造山带相接。秦岭造山带经历了多期复杂构造演化历史,记录了华北克拉通与华南克拉通的拼合,是典型的复合型大陆造山带(刘树文等,2011;孙卫东等,2000;张国伟等,2001;Dong *et al.*, 2011a, b, c, 2012a, b; Lai and Zhang, 1996; Lai *et al.*, 2004a, b;

Liu *et al.*, 2011; Meng and Zhang, 1999, 2000; Ratschbacher *et al.*, 2003; Sun and Li, 1998; Sun *et al.*, 2002; Yang *et al.*, 2011, 2012; Zhang *et al.*, 1996, 2011)。

前人将秦岭造山带划分为6个近东西向分布的构造单元,从北向南依次为:华北克拉通南缘,北秦岭构造带,商州-丹凤断裂带,南秦岭构造带,勉县-略阳断裂带,扬子克拉通北缘(图1)(刘树文等,2011;秦江锋等,2005,2007;秦江峰

* 本文受国家科技支撑计划课题(2011BAB04B05)、中国地质调查局项目(1212011085534)及国家自然科学基金(41272209,41121062,41072143)资助。

第一作者简介:阎明,男,1989年生,硕士生,地球化学专业,E-mail: yanming198903@163.com

** 通讯作者:刘树文,男,1958年生,博士,教授,岩石学和地球化学专业,E-mail: swliu@pku.edu.cn

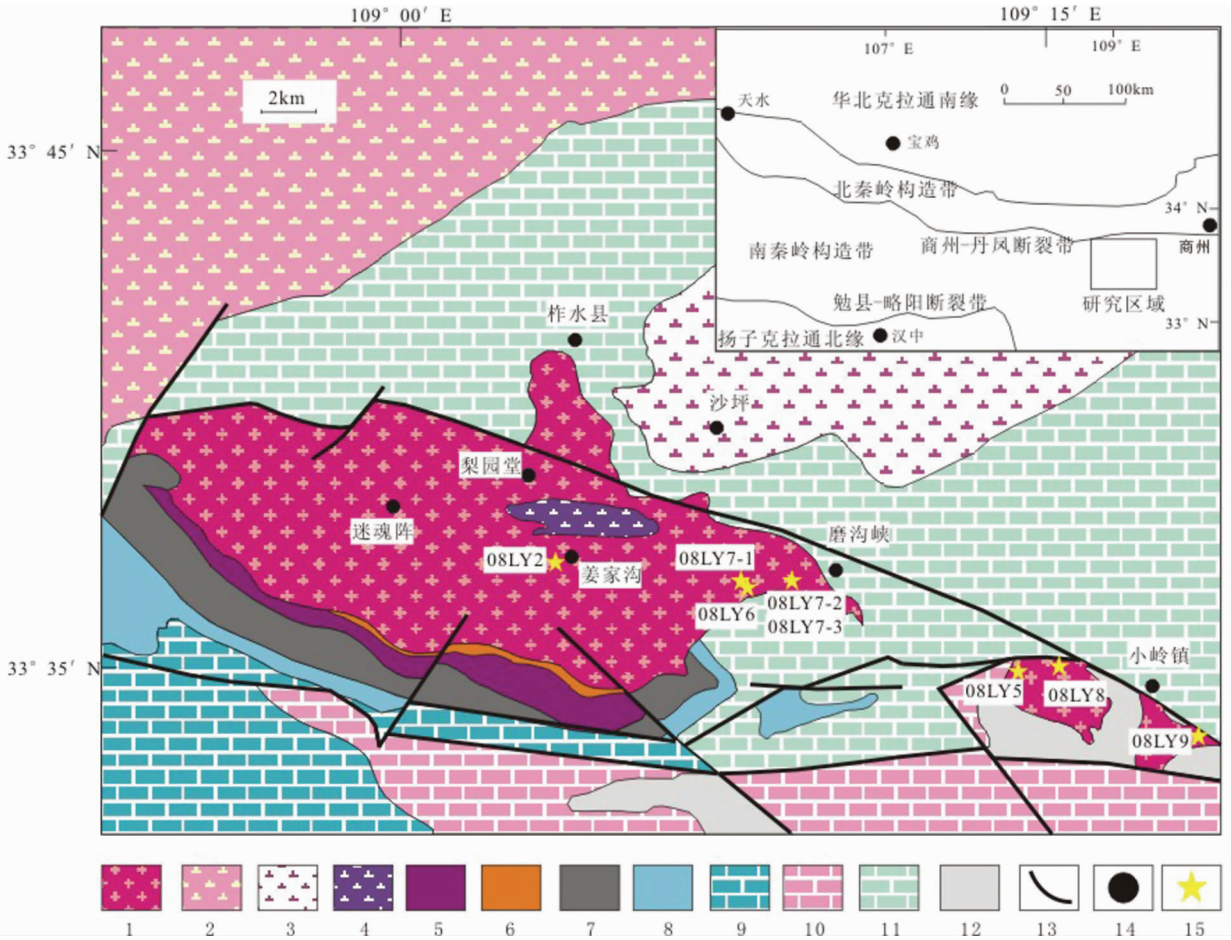


图1 迷魂阵岩体区域地质简图

1-迷魂阵岩体;2-东江口岩体;3-柞水岩体;4-梨园堂岩体;5-上震旦统陡山沱组;6-上震旦统灯影组;7-寒武系;8-奥陶系;9-中泥盆统古道岭组;10-上泥盆统九里坪组;11-上泥盆统刘岭组;12-中石炭统铁厂铺组;13-断层;14-主要村镇;15-取样位置

Fig.1 Regional geological map of the Mihunzhen pluton in southern Qinling tectonic belt, Central China

和赖少聪,2011;张国伟等,2001;Dong *et al.*, 2011a, b, c, 2012a, b; Jiang *et al.*, 2010; Liu *et al.*, 2011; Mattauer *et al.*, 1985; Meng and Zhang, 1999, 2000; Qin *et al.*, 2007, 2008a, b, 2010a, b; Zhang *et al.*, 1996)。

北秦岭构造带位于洛南-栾川断裂和商州-丹凤断裂带之间(陈岳龙等,1995),主要由前寒武地块、新元古代-早古生代蛇绿岩套、早古生代中级变质的沉积岩-火山岩、古生代-早中生代花岗质侵入体组成(刘树文等,2011;张国伟等,2001; Dong *et al.*, 2011a, b; Li *et al.*, 2009; Liu *et al.*, 2011; Qin *et al.*, 2010a; Yang *et al.*, 2012)。南秦岭构造带位于商州-丹凤断裂带和勉县-略阳断裂带之间,发育大量晚古生代沉积岩系,少量上古生界-下三叠系沉积岩系及三叠纪-侏罗纪早期花岗质侵入体(刘树文等,2011;张国伟等,2001;Dong *et al.*, 2011b; Liu *et al.*, 2011; Mattauer *et al.*, 1985; Qin *et al.*, 2010a, b; Yang *et al.*, 2012)。扬子克拉通北缘主要由一套新元古代火山-沉积岩和大量的花岗质侵入岩组成(刘树文等,2011;Liu *et al.*, 2011)。商州-丹凤断裂带作为分隔

南、北秦岭构造带的边界断层,记录了新元古代和晚古生代北向的俯冲-碰撞事件(张国伟等,2001;王宗起等,2009)。勉县-略阳断裂带则被认为代表了古特提斯洋北支的闭合的主要构造带(张国伟等,2001;Lai *et al.*, 2004a, b; Lai and Zhang, 1996; Meng and Zhang, 1999, 2000)。

近年来,在南秦岭构造带内陆续发现大量的中-新元古代的老地块,主要由变质火山-沉积岩系和古深成侵入体构成,主要分布于汉南一带,以及沿着柞水-山阳断裂南部出露的陡岭岩群等,其中汉南一带的新元古代深成侵入体表现出较弱的变形和变质特征(陆松年等,2004)。然而,目前对南秦岭构造带中柞水-山阳地区出露的中-新元古代古深成侵入体的认识还欠深入,制约了对南秦岭构造带构造演化的理解和认识。小磨岭地区出露的前寒武纪岩块与邻区佛坪、武当等地的古老岩块共同构成了南秦岭构造带前寒武纪老陆块,其岩性组成较为复杂,主要出露有基性火山岩、辉长岩、辉绿岩和中酸性侵入岩体。本文对其中的迷魂阵岩体进行了系统的地质学、岩石学、锆石 U-Pb 年代学和 Lu-Hf 同位素的系

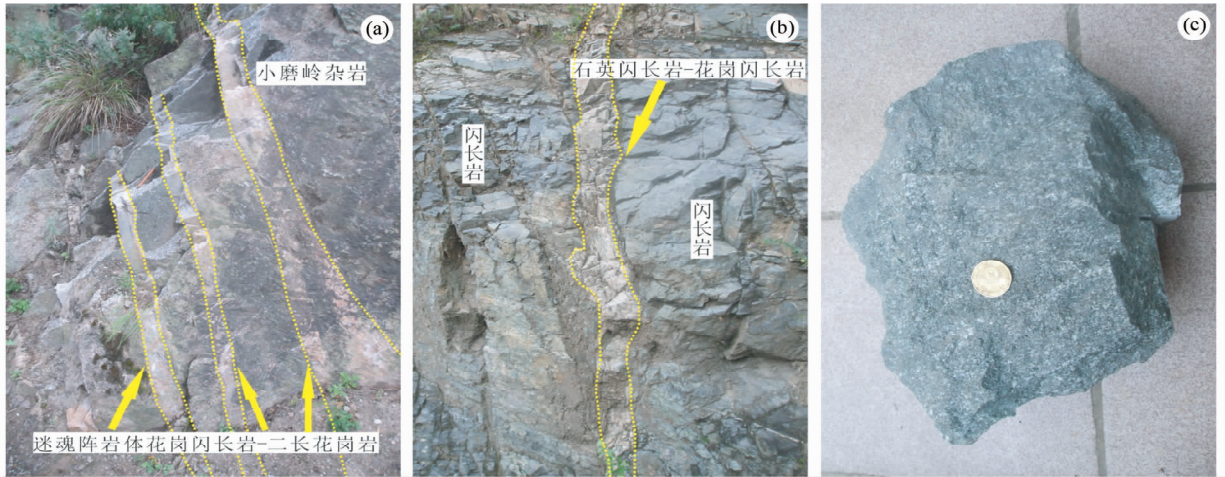


图2 迷魂阵岩体野外地质特征及手标本照片

(a)-花岗闪长岩-二长花岗岩脉侵入到小磨岭杂岩中;(b)-石英闪长岩-花岗闪长岩脉侵入到闪长岩之中;(c)-闪长岩中有浸染状磁黄铁矿、黄铜矿

Fig.2 Field and specimen photos of the Mihunzhen pluton

统研究,目的在于确定其岩石成因和区域构造意义,为深入理解南秦岭构造带的形成与演化提供老地块方面的依据。

1 地质背景和岩体特征

迷魂阵岩体主要出露于柞水县南,在柞水-山阳断裂北部,西与东江口岩体相邻,东至柞水地区的磨沟峡和小岭镇地区。该岩体呈近东西向展布,呈长椭圆形,向东被断裂分割,面积约140km²(图1)。岩体的南缘侵入到中级变质的小磨岭杂岩中,其北部、西部、东部与泥盆系地层相邻,表现为挤压破碎或断层接触(图1)。中生代梨园堂似斑状二长花岗岩-钾长花岗岩岩体侵入其中。迷魂阵岩体的岩石类型包括闪长岩、石英闪长岩、花岗闪长岩和少量二长花岗岩,主要由两期岩浆活动形成,早期阶段的闪长岩分布面积较大,其中含细粒闪长岩包体。晚期阶段的岩石主要分布在岩体的中部及东部,以石英闪长岩-花岗闪长岩为主,伴有少量的二长花岗岩,三者之间为渐变过渡关系,侵入到早期阶段的闪长岩之中(图2a, b)。其中闪长岩通常发生磁黄铁矿化和铜矿化,磁黄铁矿和黄铜矿以浸染状或微细脉状产出(图2c)。

迷魂阵岩体的南部围岩是小磨岭杂岩的火山-沉积岩系。该岩系主要由基性火山岩、陆源碎屑岩、辉长-辉绿岩,闪长岩和花岗岩,多遭受绿片岩相-低角闪岩相变质作用,之上被上震旦统陡山沱组和灯影组不整合覆盖。它们均被泥盆系和少量寒武系-奥陶系-石炭系沉积盖层覆盖,以断裂或断裂带接触(杨钊等,2008)。陡山沱组下部为砂砾岩,上部为石英砂岩、钙质砂岩与微粒灰岩互层。刘鹏举等(2009)对陡山沱组中部暴露间断面之下火山岩进行了锆石 SHRIMP U-Pb 年龄测定,获得了陡山沱组的沉积时代为614 ± 8Ma;灯影组下部为白云质灰岩、白云岩夹少量薄层状含泥质微粒灰

岩,上部为厚层硅质白云质灰岩及白云岩。显生宙盖层从底部到顶部依次为寒武系(C₁)炭质千枚岩、铝土质页岩、泥质白云质灰岩、硅质白云质灰岩;奥陶系(O)白云质结晶灰岩、燧石灰岩夹泥质灰岩条带;中泥盆统(D₂)古道岭组黑云母石英片岩、结晶灰岩、石英岩、炭质硅质岩及大理岩;上泥盆统(D₃)九里坪组砂质板岩、变质砂岩、钙质板岩与泥质灰岩;中石炭统(C₂)铁厂铺群千枚岩、钙质千枚岩及灰岩。

研究区北部、西部、东部主要为泥盆纪刘岭群沉积岩系(图1),由上泥盆统桐峪寺组和下东沟组、中泥盆统牛耳川组、池沟组和青石垭组组成。桐峪寺组为一套浅海相沉积建造,主要由石英砂岩、石英长石砂岩、钙质砂岩和石灰岩组成。下东沟组、牛耳川组、池沟组和青石垭组为潮坪相组合,下东沟组主要由泥质板岩、钙质粉砂岩和泥质粉砂岩组成;牛耳川组主要由细粒砂岩、粉砂岩、泥-砂质板岩和少量白云石灰岩组成;池沟组主要由细粒砂岩、泥质粉砂岩、钙质泥岩和石灰岩组成;青石垭组由粉砂岩、泥岩和石灰岩组成(杜定汉,1986;闫臻等,2007;Yan *et al.*, 2006, 2012)。

2 样品特征及分析方法

2.1 样品特征描述

本文选择3件代表性样品进行了LA-ICP-MS 锆石 U-Pb 同位素年代学分析,其中样品08LY2-8采于姜家沟,为迷魂阵岩体早期阶段的闪长岩,地理坐标为N33°36'24",E109°04'10";样品08LY6-1取自磨沟峡,为晚期阶段的石英闪长岩,地理坐标为N33°35'52",E109°09'55";样品08LY8-3取自小岭镇附近,为晚期阶段的花岗闪长岩,地理坐标为N33°34'33",E109°15'45"。

早期阶段侵位的闪长岩为中-细粒半自形粒状结构,块状构造,主要矿物为斜长石(50%~55%)、钾长石(2%~5%)、角闪石(20%~25%)、辉石(5%~10%)、石英(1%~

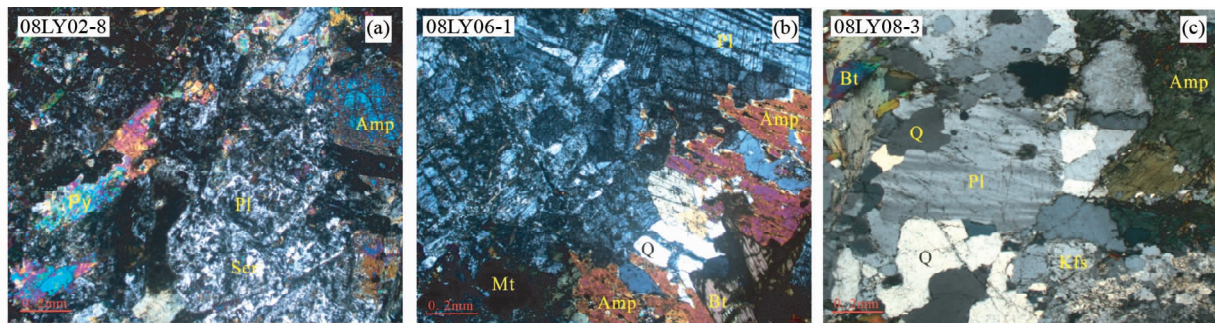


图3 迷魂阵岩体样品显微照片(正交偏光)

Ser-绢云母;Bt-黑云母;Amp-角闪石;Pl-斜长石;Kfs-钾长石;Q-石英;Mt-磁铁矿

Fig.3 Micrographs of samples from the Mihunzhen pluton (cross polarized light)

Ser-sericite; Bt-biotite; Amp-amphibole; Pl-plagioclase; Kfs-K-feldspar; Q-quartz; Mt-magnetite

3%)，副矿物为锆石、磷灰石(图3a)。晚期阶段侵位的石英闪长岩的结构为中粒,半自形粒状结构,块状构造,其中斜长石(55%~60%)、钾长石(~5%)、角闪石(15%~20%)、黑云母(5%)、石英(10%~15%)，副矿物为磁铁矿、锆石、磷灰石(图3b);花岗闪长岩为中-粗粒不等粒花岗结构,块状构造,主要矿物为斜长石(45%~50%)、石英(15%~20%)、钾长石(10%)，暗色矿物为黑云母(10%)和角闪石(5%)，副矿物为磁铁矿、锆石、磷灰石(图3c)。

2.2 分析方法

各样品的锆石单矿物分离是在河北区测队(廊坊)完成,将大约5kg重的样品破碎到60~80目,经常规浮选和磁选方法分选后,在双目镜下挑纯。将挑纯的锆石颗粒粘在双面胶上,然后用无色透明的环氧树脂固定,待环氧树脂充分固化后抛磨至粒径的大约二分之一,使锆石内部结构充分暴露,然后进行锆石显微(反射光、透射光和CL图像)照相。锆石的显微照相在北京大学电子学系及物理学系扫描电镜上完成。

锆石的U-Th-Pb及Lu-Hf同位素测试均在西北大学大陆动力学国家重点实验室完成。锆石定年分析所用的ICP-MS是Agilent公司最新一代的带有Shield Torch的Agilent 7500a。原位锆石Lu-Hf同位素测定采用Nu Plasma HR(Wrexham, UK)多接收电感耦合等离子体质谱仪完成(MC-ICP-MS)。采用的激光剥蚀系统为德国MicroLas公司生产的GeoLas200M,该系统由德国Lambda Physik公司的ComPex102 Excimer激光器(波长193nm)与MicroLas公司的光学系统组成(第五春荣等,2008,2010)。

3 分析结果

3.1 锆石 U-Pb 年龄

3.1.1 样品 08LY2-8(闪长岩)

样品08LY2-8为迷魂阵岩体早期阶段侵位的闪长岩,共对其进行了25颗锆石25个点的LA-ICP-MS U-Pb同位素分

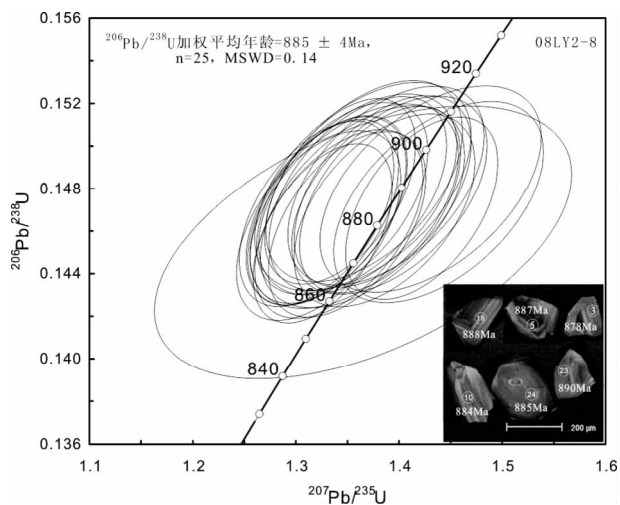


图4 闪长岩(08LY2-8)的锆石特征和U-Pb年龄图

Fig.4 The zircon U-Pb isotopic concordia diagram and CL images of representative zircon grains from early diorite sample (08LY2-8)

析。CL图像显示大多数锆石颗粒为半自形-自形短柱状晶形,长度在100~200μm之间,长宽比在1:1到2:1之间,具有震荡环带或扇形带,应属于岩浆成因锆石(图4)。其Th/U比为0.45~0.96,²⁰⁶Pb/²³⁸U表观年龄为876~892Ma(表1)。在²⁰⁷Pb/²³⁵U-²⁰⁶Pb/²³⁸U的谐和图(图4)上,所有分析点全部落在谐和线上或者附近,其²⁰⁶Pb/²³⁸U加权平均年龄为885±4Ma(图4),MSWD=0.14,代表了早期阶段闪长质岩浆侵位年龄。

3.1.2 样品 08LY6-1(石英闪长岩)

样品08LY6-1为迷魂阵岩体晚期阶段侵位的石英闪长岩,共对其进行了18颗锆石18个点的LA-ICP-MS U-Pb同位素分析。在CL图像中这些被分析的锆石表现为灰黑色,不具备明显的振荡环带,多数为长柱状,长度在80~300μm之间,颗粒的长宽比变化较大,为3:2~7:2,其Th/U比0.91~1.21,为岩浆锆石。其²⁰⁶Pb/²³⁸U表观年龄比较集中,为734

表1 锆石 U-Th-Pb 同位素分析数据和年龄值

Table 1 Analytical data of zircon U-Th-Pb isotopes and age values

测点号	Th/U	$^{207}\text{Pb}/^{206}\text{Pb}$	1 σ	$^{207}\text{Pb}/^{235}\text{U}$	1 σ	$^{206}\text{Pb}/^{238}\text{U}$	1 σ	$^{207}\text{Pb}/^{235}\text{U}$ 年龄 (Ma)	1 σ	$^{206}\text{Pb}/^{238}\text{U}$ 年龄 (Ma)	1 σ
闪长岩											
08LY2-8-01	0.51	0.06457	0.00096	1.32212	0.03258	0.14627	0.00182	847	14	880	10
08LY2-8-02	0.48	0.06521	0.00087	1.32015	0.03066	0.14682	0.00178	855	13	883	10
08LY2-8-03	0.96	0.06542	0.00076	1.32598	0.02757	0.1459	0.00172	853	12	878	10
08LY2-8-04	0.71	0.0669	0.00089	1.34975	0.03121	0.14632	0.00178	867	13	880	10
08LY2-8-05	0.49	0.06794	0.0009	1.38159	0.0319	0.14748	0.00179	881	14	887	10
08LY2-8-06	0.71	0.06471	0.0009	1.33184	0.03124	0.14702	0.0018	851	14	884	10
08LY2-8-07	0.79	0.06352	0.00085	1.32655	0.02992	0.14689	0.00178	840	13	884	10
08LY2-8-08	0.45	0.07012	0.00082	1.42208	0.0302	0.14708	0.00175	898	13	885	10
08LY2-8-09	0.78	0.06562	0.00083	1.34294	0.02994	0.14787	0.00178	862	13	889	10
08LY2-8-10	0.77	0.06413	0.00092	1.32941	0.03175	0.14695	0.00181	845	14	884	10
08LY2-8-11	0.51	0.0665	0.00098	1.34185	0.03337	0.14634	0.00181	864	14	880	10
08LY2-8-12	0.52	0.06838	0.00106	1.38597	0.03588	0.14698	0.00185	883	15	884	10
08LY2-8-13	0.67	0.06675	0.00104	1.36009	0.03525	0.14777	0.00186	872	15	888	10
08LY2-8-14	0.62	0.06611	0.00099	1.34501	0.03396	0.14754	0.00184	865	15	887	10
08LY2-8-15	0.8	0.06789	0.00103	1.38427	0.03509	0.14787	0.00184	882	15	889	10
08LY2-8-16	0.83	0.06679	0.00119	1.36634	0.03899	0.14835	0.00193	875	17	892	11
08LY2-8-17	0.53	0.06792	0.00118	1.38737	0.03893	0.14814	0.00191	884	17	891	11
08LY2-8-18	0.46	0.06677	0.00121	1.36008	0.03933	0.14772	0.00193	872	17	888	11
08LY2-8-19	0.45	0.06829	0.00118	1.39072	0.03877	0.14769	0.0019	885	16	888	11
08LY2-8-20	0.76	0.07077	0.00127	1.43825	0.04151	0.14737	0.00193	905	17	886	11
08LY2-8-21	0.69	0.06726	0.00126	1.36473	0.04049	0.14715	0.00194	874	17	885	11
08LY2-8-22	0.51	0.06806	0.00302	1.36516	0.08255	0.14547	0.00262	874	35	876	15
08LY2-8-23	0.73	0.06685	0.00135	1.36503	0.04288	0.14809	0.002	874	18	890	11
08LY2-8-24	0.83	0.06685	0.00129	1.3567	0.04127	0.14718	0.00196	870	18	885	11
08LY2-8-25	0.47	0.0701	0.00136	1.43046	0.04377	0.14798	0.00198	902	18	890	11
石英闪长岩											
08LY6-1-01	1.14	0.05859	0.00139	1.05319	0.023	0.12171	0.00147	696	12	737	8
08LY6-1-02	1.11	0.05856	0.00157	1.05122	0.02586	0.12154	0.00151	695	13	739	9
08LY6-1-03	1.06	0.05927	0.00142	1.06514	0.02351	0.12169	0.00146	702	12	737	8
08LY6-1-04	1.15	0.05827	0.00131	1.05183	0.02174	0.12223	0.00144	695	11	743	8
08LY6-1-05	1.21	0.05881	0.00135	1.06115	0.02245	0.12219	0.00145	700	11	743	8
08LY6-1-06	1.1	0.05774	0.0014	1.03412	0.02291	0.12133	0.00144	687	12	738	8
08LY6-1-07	1.16	0.0618	0.0017	1.09938	0.02751	0.12053	0.00149	718	14	734	9
08LY6-1-08	1.18	0.05869	0.00132	1.05522	0.02164	0.12183	0.00141	697	11	741	8
08LY6-1-09	1.26	0.05836	0.00136	1.04319	0.02209	0.12116	0.00141	691	11	737	8
08LY6-1-10	0.91	0.06075	0.00177	1.10330	0.02918	0.12312	0.00154	720	15	749	9
08LY6-1-11	1.18	0.05922	0.0015	1.07198	0.02456	0.12275	0.00146	705	12	746	8
08LY6-1-12	1.14	0.06017	0.00163	1.08357	0.02648	0.12212	0.00148	710	13	743	8
08LY6-1-13	1.19	0.05867	0.00154	1.04486	0.02467	0.1208	0.00144	692	13	735	8
08LY6-1-14	1.21	0.06033	0.00168	1.07515	0.02655	0.12101	0.00146	706	13	736	8
08LY6-1-15	1.18	0.0582	0.00164	1.04072	0.02608	0.12144	0.00146	690	13	739	8
08LY6-1-16	1.19	0.0605	0.00164	1.08130	0.02584	0.12141	0.00144	709	13	739	8
08LY6-1-17	1.15	0.0585	0.00182	1.04587	0.02886	0.12147	0.00151	692	15	739	9
08LY6-1-18	1.18	0.0603	0.00171	1.08287	0.02688	0.12204	0.00146	710	14	742	8
花岗闪长岩											
08LY8-3-01	1.54	0.06102	0.0015	1.00183	0.03628	0.11906	0.00164	705	18	725	9
08LY8-3-02	1.3	0.0688	0.00213	1.15301	0.05113	0.12153	0.00191	779	24	739	11
08LY8-3-03	0.88	0.06611	0.00078	1.12232	0.02357	0.12309	0.00142	764	11	748	8
08LY8-3-04	1.43	0.06263	0.00167	1.0558	0.04101	0.12223	0.00175	732	20	743	10
08LY8-3-05	1.47	0.12677	0.00208	2.08137	0.05726	0.11904	0.00162	1143	19	725	9

续表 1

Continued Table 1

测点号	Th/U	$^{207}\text{Pb}/^{206}\text{Pb}$	1σ	$^{207}\text{Pb}/^{235}\text{U}$	1σ	$^{206}\text{Pb}/^{238}\text{U}$	1σ	$^{207}\text{Pb}/^{235}\text{U}$ 年龄 (Ma)	1σ	$^{206}\text{Pb}/^{238}\text{U}$ 年龄 (Ma)	1σ
08LY8-3-06	1.3	0.06167	0.00141	0.97686	0.03346	0.11483	0.00156	692	17	701	9
08LY8-3-07	0.76	0.0612	0.00101	1.02551	0.02743	0.12148	0.00151	717	14	739	9
08LY8-3-08	0.9	0.0633	0.0009	1.06633	0.0257	0.12213	0.00148	737	13	743	9
08LY8-3-09	1.59	0.06129	0.00123	1.02376	0.032	0.12109	0.00161	716	16	737	9
08LY8-3-10	1.37	0.06077	0.00168	1.00762	0.04053	0.1202	0.00178	708	20	732	10
08LY8-3-11	1.28	0.06091	0.00135	1.02775	0.0347	0.12233	0.00169	718	17	744	10
08LY8-3-12	1.02	0.05911	0.00163	0.99791	0.03935	0.11994	0.00179	693	20	730	10
08LY8-3-13	2.13	0.06014	0.00125	1.02019	0.0319	0.11963	0.00163	700	16	728	9
08LY8-3-14	1.75	0.06577	0.0017	1.10212	0.04255	0.12149	0.00183	754	21	739	11
08LY8-3-15	1.06	0.07081	0.0016	1.16662	0.04159	0.12254	0.00177	799	19	745	10
08LY8-3-16	1.54	0.06119	0.0016	0.96873	0.03798	0.11483	0.00177	688	20	701	10
08LY8-3-17	1.14	0.0593	0.00165	0.97055	0.03997	0.11871	0.00187	689	21	723	11
08LY8-3-18	1.49	0.05832	0.00152	1.03944	0.03825	0.12182	0.00189	693	20	741	11
08LY8-3-19	0.94	0.06144	0.00161	1.03154	0.04059	0.12181	0.00191	720	20	741	11
08LY8-3-20	1.59	0.0591	0.00162	0.99749	0.04051	0.12123	0.00195	697	21	738	11
08LY8-3-21	1.1	0.05965	0.00162	1.01092	0.04038	0.12054	0.00195	699	21	734	11
08LY8-3-22	1.09	0.05666	0.002	1.01384	0.04788	0.12089	0.00218	675	25	736	13
08LY8-3-23	1.72	0.05931	0.00193	1.0221	0.04711	0.1214	0.00213	700	24	739	12

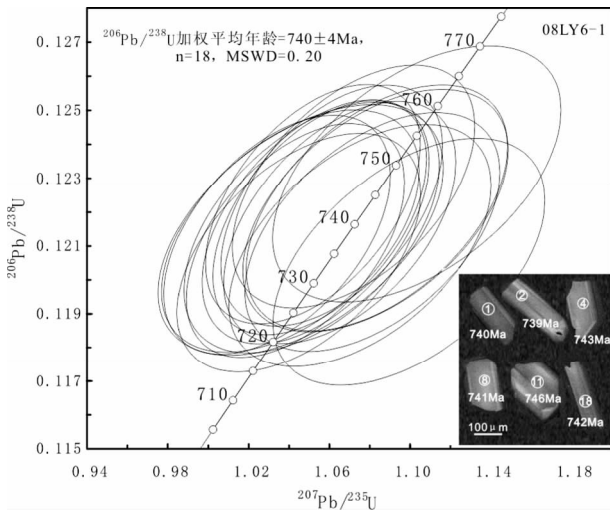


图 5 石英闪长岩 (08LY06-1) 的锆石特征和 U-Pb 年龄图

Fig. 5 The zircon U-Pb isotopic concordia diagram and CL images of representative zircon grains from late quartz diorite sample (08LY06-1)

~749Ma (表 1)。在 $^{207}\text{Pb}/^{235}\text{U}$ - $^{206}\text{Pb}/^{238}\text{U}$ 构建的谐和图中 (图 5), 分析点均落于谐和线上, 获得的 $^{206}\text{Pb}/^{238}\text{U}$ 加权平均年龄为 $740 \pm 4\text{Ma}$ (图 5), $\text{MSWD} = 0.20$, 代表晚期阶段岩浆侵位年龄。

3.1.3 样品 08LY8-3 (花岗闪长岩)

样品 08LY8-3 为迷魂阵岩体晚期侵位的花岗闪长岩, 共对其进行了 23 颗锆石 23 个点的 LA-ICP-MS U-Pb 同位素分

析。锆石在 CL 图像中表现为短柱状, 具备明显的振荡环带, 长度在 $100 \sim 200\mu\text{m}$ 之间, 颗粒的长宽比变化不大, 为 $1 : 1 \sim 3 : 2$, 其 Th/U 比 $0.76 \sim 2.13$, 为岩浆锆石。其中分析点 5 远离谐和线, 分析点 6 和 16 给出较小的 $^{206}\text{Pb}/^{238}\text{U}$ 表观年龄 701Ma, 并表现为不谐和, 故年龄计算中没有使用。其它 20 个分析点的 $^{206}\text{Pb}/^{238}\text{U}$ 表观年龄为 $723 \sim 748\text{Ma}$ (表 1), 在 $^{207}\text{Pb}/^{235}\text{U}$ - $^{206}\text{Pb}/^{238}\text{U}$ 谐和图 (图 6) 中均落于谐和线上及其附近, 获得了 $737 \pm 4\text{Ma}$ 的 $^{206}\text{Pb}/^{238}\text{U}$ 加权平均年龄 (图 6), MSWD

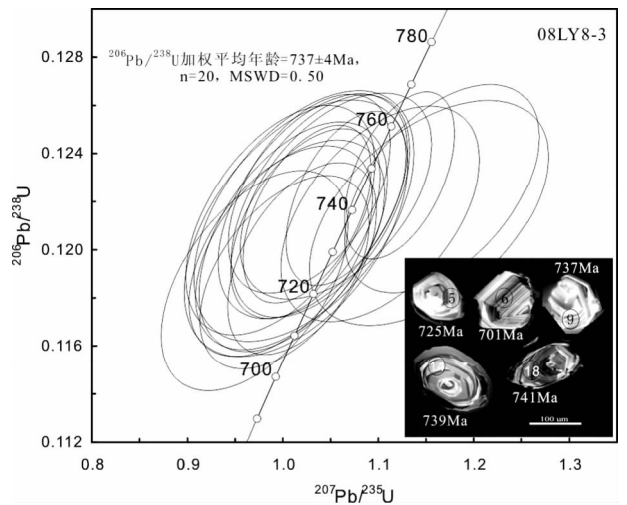


图 6 花岗闪长岩 (08LY8-3) 的锆石特征和 U-Pb 年龄图

Fig. 6 The zircon U-Pb isotopic concordia diagram and CL images of representative zircon grains from late granodiorite sample (08LY8-3)

表2 LA-MC-ICPMS 锆石 Lu-Hf 同位素分析结果

Table 2 LA-MC-ICPMS zircon Lu-Hf isotopic compositions

测点号	Age(Ma)	$^{176}\text{Yb}/^{177}\text{Hf}$	$^{176}\text{Lu}/^{177}\text{Hf}$	$^{176}\text{Hf}/^{177}\text{Hf}$	2s	$^{176}\text{Hf}/^{177}\text{Hf}_i$	$\varepsilon_{\text{Hf}}(0)$	$\varepsilon_{\text{Hf}}(t)$	$t_{\text{DM}}(\text{Ma})$	$f_{\text{Lu/Hf}}$
闪长岩										
08LY2-8-1		0.013315	0.000535	0.282531	0.000031	0.282521899	-8.5	10.7	1008	-0.98
08LY2-8-2		0.016358	0.000671	0.282417	0.000034	0.282405819	-12.6	6.6	1170	-0.98
08LY2-8-3		0.042303	0.001607	0.282514	0.000032	0.282486924	-9.1	9.5	1061	-0.95
08LY2-8-4		0.020043	0.000766	0.282510	0.000026	0.282497423	-9.3	9.9	1043	-0.98
08LY2-8-5		0.017149	0.000683	0.282571	0.000027	0.282559766	-7.1	12.1	955	-0.98
08LY2-8-6		0.015850	0.000625	0.282513	0.000033	0.282502199	-9.2	10.0	1035	-0.98
08LY2-8-7		0.026065	0.000959	0.282489	0.000026	0.282472655	-10.0	9.0	1078	-0.97
08LY2-8-8		0.018466	0.000732	0.282419	0.000023	0.282406912	-12.5	6.7	1169	-0.98
08LY2-8-9		0.025621	0.000936	0.282502	0.000024	0.282486826	-9.5	9.5	1058	-0.97
08LY2-8-10		0.024549	0.000895	0.282477	0.000028	0.282462233	-10.4	8.6	1093	-0.97
08LY2-8-11		0.021516	0.000817	0.282574	0.000021	0.28256084	-7.0	12.1	954	-0.98
08LY2-8-12		0.018078	0.000682	0.282514	0.000027	0.282502383	-9.1	10.0	1035	-0.98
08LY2-8-13	885	0.019667	0.000738	0.282472	0.000021	0.282459356	-10.6	8.5	1096	-0.98
08LY2-8-14		0.022915	0.000868	0.282534	0.000024	0.282519808	-8.4	10.7	1012	-0.97
08LY2-8-15		0.029904	0.001130	0.282507	0.000024	0.282488534	-9.4	9.6	1057	-0.97
08LY2-8-16		0.029607	0.001072	0.282518	0.000025	0.28250061	-9.0	10.0	1040	-0.97
08LY2-8-17		0.015575	0.000593	0.282473	0.000020	0.282462791	-10.6	8.6	1090	-0.98
08LY2-8-18		0.016647	0.000639	0.282477	0.000022	0.282466737	-10.4	8.8	1085	-0.98
08LY2-8-19		0.023686	0.000937	0.282520	0.000025	0.282504566	-8.9	10.1	1033	-0.97
08LY2-8-20		0.021313	0.000767	0.282548	0.000024	0.282534993	-7.9	11.2	990	-0.98
08LY2-8-21		0.020493	0.000752	0.282499	0.000019	0.282486602	-9.6	9.5	1058	-0.98
08LY2-8-22		0.013009	0.000487	0.282567	0.000021	0.282559031	-7.2	12.1	956	-0.99
08LY2-8-23		0.019696	0.000704	0.282492	0.000026	0.282479977	-9.9	9.3	1067	-0.98
08LY2-8-24		0.034223	0.001193	0.282538	0.000026	0.282517957	-8.3	10.6	1016	-0.96
08LY2-8-25		0.015933	0.000606	0.282525	0.000022	0.28251513	-8.7	10.5	1017	-0.98
石英闪长岩										
08LY6-1-2		0.035597	0.001292	0.282468	0.000024	0.282450347	-10.7	5.0	1117	-0.96
08LY6-1-3		0.036074	0.001293	0.282442	0.000030	0.282423919	-11.7	4.0	1154	-0.96
08LY6-1-4		0.043024	0.001518	0.282372	0.000034	0.282350704	-14.2	1.4	1260	-0.95
08LY6-1-5		0.044268	0.001599	0.282504	0.000032	0.282481604	-9.5	6.1	1075	-0.95
08LY6-1-6		0.043423	0.001577	0.282445	0.000032	0.282422665	-11.6	4.0	1159	-0.95
08LY6-1-7		0.040636	0.001468	0.282412	0.000038	0.282392043	-12.7	2.9	1201	-0.96
08LY6-1-8		0.041335	0.001486	0.282586	0.000029	0.282565047	-6.6	9.0	955	-0.96
08LY6-1-9		0.045432	0.001660	0.282536	0.000030	0.282512672	-8.4	7.2	1031	-0.95
08LY6-1-10	740	0.056541	0.002013	0.282569	0.000031	0.282540518	-7.2	8.2	994	-0.94
08LY6-1-11		0.026412	0.000965	0.282447	0.000025	0.282433398	-11.5	4.4	1137	-0.97
08LY6-1-12		0.049586	0.001782	0.282437	0.000033	0.282412409	-11.8	3.6	1176	-0.95
08LY6-1-13		0.042446	0.001522	0.282438	0.000030	0.282416852	-11.8	3.8	1167	-0.95
08LY6-1-14		0.044495	0.001590	0.282555	0.000035	0.282532639	-7.7	7.9	1002	-0.95
08LY6-1-15		0.039624	0.001426	0.282517	0.000031	0.282496909	-9.0	6.6	1052	-0.96
08LY6-1-16		0.046446	0.001666	0.282498	0.000024	0.282474691	-9.7	5.8	1086	-0.95
08LY6-1-17		0.039666	0.001439	0.282456	0.000028	0.282435681	-11.2	4.4	1139	-0.96
08LY6-1-18		0.047452	0.001689	0.282455	0.000030	0.282431456	-11.2	4.3	1148	-0.95

=0.50,代表该样品岩浆侵位年龄,与石英闪长岩的侵位年龄在误差范围内一致,因此迷魂阵岩体中石英闪长岩-花岗闪长岩的形成时代为 $740 \pm 4\text{Ma}$ 。

3.2 锆石 Hf 同位素

根据样品地质和锆石 U-Pb 年代学特征,对分别代表先

后两个不同阶段的样品 08LY2-8 和 08LY6-1 进行了锆石原位 Lu-Hf 同位素的测试,数据列于表 2,并表示于图 7。

早期阶段侵位的闪长岩样品 08LY2-8 共进行了 25 个点的 Lu-Hf 同位素分析,用样品的结晶年龄 (885Ma) 对 $^{176}\text{Hf}/^{177}\text{Hf}$ 和 $\varepsilon_{\text{Hf}}(t)$ 值进行校正,得出闪长岩的初始 $^{176}\text{Hf}/^{177}\text{Hf}$ 值为 0.0282406 ~ 0.0282561, $\varepsilon_{\text{Hf}}(t)$ 值为 +6.6 ~ +12.1,平均

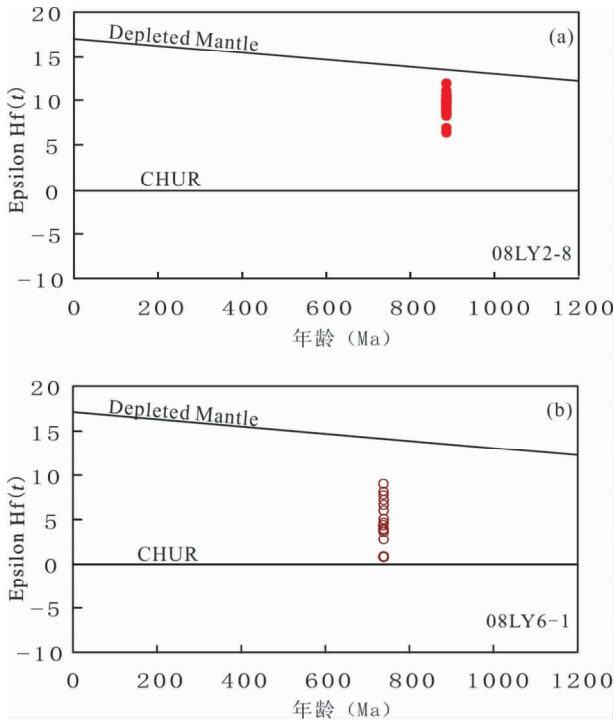


图7 迷魂阵岩体 Hf 同位素特征

(a)-闪长岩(08LY2-8);(b)-石英闪长岩(08LY6-1)

Fig.7 In-situ zircon Hf isotopic data of Mihunzhen pluton

(a)-diorite (08LY2-8); (b)-quartz diorite (08LY6-1)

值为 +9.8, Hf 同位素模式年龄 (t_{DM}) 为 955 ~ 1170Ma, 平均值为 1047Ma, 与岩浆结晶年龄接近(图 7a), 揭示了闪长质岩浆主要源于亏损地幔, 岩浆侵位结晶过程中可能受到了地壳物质的混染。

晚期阶段侵位的石英闪长岩样品 08LY6-1 共进行了 18 个点的 Lu-Hf 同位素分析, 用 740Ma 的结晶年龄校正后的初始 $^{176}\text{Hf}/^{177}\text{Hf}$ 值为 0.0282351 ~ 0.0282565, $\epsilon_{\text{Hf}}(t)$ 值为 +1.4 ~ +9.0, 平均值为 +5.0, t_{DM} 为 955 ~ 1260Ma, 平均值为 1119Ma(图 7b), 表现出以亏损地幔源岩浆为主受到了元古代地壳物质的混染。

4 讨论

3 个样品的 LA-ICP-MS 锆石 U-Pb 定年结果表明迷魂阵岩体形成于两个岩浆阶段, 早期岩浆阶段形成闪长岩, 其年龄为 $885 \pm 4\text{Ma}$; 晚期岩浆阶段形成石英闪长岩-花岗闪长岩, 时代为 $\sim 740 \pm 4\text{Ma}$ 。早期阶段侵入的闪长岩的年龄与出露于扬子克拉通北缘的铜厂闪长岩体侵位时代 ($879 \pm 7\text{Ma}$, 王伟等, 2010; Wang *et al.*, 2012) 基本一致, 位于扬子陆块核部的三斗坪英云闪长岩具有 $795 \pm 8\text{Ma}$ 的结晶年龄, 五堵门岩体英云闪长岩侵位于 $789 \pm 10\text{Ma}$ (凌文黎, 2006)。这些年代学证据说明南秦岭构造带内的一些老地块与扬子克拉通北缘及内部新元古代时期有相似的岩浆活动历史, 因此南秦岭

构造带内一些老地块或者属于扬子克拉通新元古代结晶基底的一部分, 或者是从扬子克拉通北缘分离出来的老地块。Li *et al.* (2008) 指出 Rodinia 超大陆拼合于 1100 ~ 900Ma, 之后约 40Myr (860 ~ 750Ma), 地幔物质上涌, 诱发相关的大陆裂谷作用和地幔柱活动。迷魂阵岩体的形成时间与 Rodinia 超大陆的主要裂解时期不一致, 可能形成于新元古代与俯冲相关的伸展背景(耿元生等, 2008; 刘树文等, 2009a, b; Zhou *et al.*, 2002, 2006; Zhao and Zhou, 2009; Zhao *et al.*, 2010, 2011)。

在 $\epsilon_{\text{Hf}}(t)$ -年龄图解中(图 7), 早期阶段的闪长岩样品(08LY2-8)的 $\epsilon_{\text{Hf}}(t)$ 值范围 +6.6 ~ +12.1, 平均值为 +9.8, 接近亏损地幔演化线, 说明早期阶段岩浆主要来自于亏损地幔物质的部分熔融。而晚期阶段石英闪长岩样品(08LY06-1)的 $\epsilon_{\text{Hf}}(t)$ 范围为 +1.4 ~ +9.0, 仍说明亏损地幔是岩浆的主要来源之一, 而壳源物质可能是制约岩浆作用的另一个重要因素, 或者形成于早期阶段闪长质岩浆的结晶分异, 之后又经地壳物质的混染, 或者形成于闪长质结晶分异的岩浆与壳源岩浆的混合作用。

5 结论

通过对迷魂阵岩体 LA-MC-ICPMS 锆石 U-Pb 同位素年代学、Lu-Hf 同位素分析, 本文得出以下认识:

(1) 迷魂阵岩体主要由闪长岩、石英闪长岩和花岗闪长岩组成, 形成于两个岩浆作用阶段, 早期阶段的闪长岩的形成时代为 $885 \pm 4\text{Ma}$, 晚期阶段的石英闪长岩-花岗闪长岩的形成时代为 $\sim 740 \pm 4\text{Ma}$ 。

(2) 早期闪长质岩浆主要来源于亏损地幔的部分熔融, 晚期石英闪长岩-花岗闪长岩岩浆主要形成于早期闪长质岩浆的结晶分异, 并经历了地壳物质的混染或者来源于壳源岩浆的混合作用。

致谢 样品的 LA-ICPMS 锆石 U-Pb 和 Lu-Hf 同位素测试得到了西北大学大陆动力学国家重点实验室袁洪林教授的支持和帮助; 主微量元素测试获得了北京大学造山带与地壳演化教育部重点实验室杨斌老师、古丽冰老师的帮助; 在此一并表示衷心的感谢。

References

Chen YL, Zhang BR and Parat A. 1995. Geochemical characteristics of Pb, Sr and Nd isotopes on Early Palaeozoic granites in the Danfeng region, northern Qinling Belt. *Earth Science*, 30(3): 247 - 258 (in Chinese with English abstract)

Diwu CR, Sun Y, Yuan HL, Wang HL, Zhong XP and Liu XM. 2008. The U-Pb chronology of detrital zircon of quartzite and its geological significance of Songshan, Denfeng area of Henan Province. *Chinese Science Bulletin*, 53(16): 1923 - 1934 (in Chinese)

Diwu CR, Sun Y, Liu L, Zhang CL and Wang HL. 2010. The

- disintegration of Kuanping Group in North Qinling orogenic belts and Neo-proterozoic N-MORB. *Acta Petrologica Sinica*, 26(16): 2025–2038 (in Chinese with English abstract)
- Dong YP, Genser J, Neubauer F, Zhang GW, Liu XM, Yang Z and Heberer B. 2011a. U-Pb and $^{40}\text{Ar}/^{39}\text{Ar}$ geochronological constraints on the exhumation history of the North Qinling terrane, China. *Gondwana Research*, 19(4): 881–893
- Dong YP, Zhang GW, Hauzenberger C, Neubauer F, Yang Z and Liu XM. 2011b. Palaeozoic tectonics and evolutionary history of the Qinling orogen, evidence from geochemistry and geochronology of ophiolite and related volcanic rocks. *Lithos*, 122(1–2): 39–56
- Dong YP, Zhang GW and Neubauer F. 2011c. Tectonic evolution of the Qinling orogen, China: Review and Synthesis. *Journal of Asian Earth Sciences*, 41(3): 213–237
- Dong YP, Liu XM, Santosh M, Chen Q, Zhang XM, Li W, He DF and Zhang GW. 2012a. Neoproterozoic accretionary tectonics along the northwestern margin of the Yangtze Block, China: Constraints from zircon U-Pb geochronology and geochemistry. *Precambrian Research*, 196–197: 247–274
- Dong YP, Liu XM, Zhang GW, Chen Q, Zhang XN, Li W and Yang C. 2012b. Triassic diorites and granitoids in the Foping area: Constraints on the conversion from subduction to collision in the Qinling Orogen, China. *Journal of Asian Earth Sciences*, 47(30): 123–142
- Du DH. 1986. Study of the Devonian of the Qinba Area, Shaanxi Province. Xian: Xi'an Jiaotong University Press, 1–230 (in Chinese)
- Geng YS, Yang CH, Wang XS, Du LL, Ren LD and Zhou XW. 2008. Evolution of Metamorphosed Basement, Yangtze Craton. Beijing: Geological Publishing House, 1–215 (in Chinese)
- Jiang YH, Jin GD, Liao SY, Zhou Q and Zhao P. 2010. Geochemical and Sr-Nd-Hf isotopic constraints on the origin of Late Triassic granitoids from the Qinling orogen, central China, implications for a continental arc to continent-continent collision. *Lithos*, 117(1–4): 183–197
- Lai SC and Zhang GW. 1996. Geochemical features of ophiolites in Mianxian-Lueyang suture zone, Qinling Orogenic Belt. *Geological Journal of China University*, 7(2): 165–172
- Lai SC, Zhang GW, Dong YP, Pei XZ and Chen L. 2004a. Geochemistry and regional distribution of ophiolite and associated volcanic rocks in Mianlue suture, Qinling-Dabie Mountains. *Science in China (Series D)*, 47(4): 289–299
- Lai SC, Zhang GW and Li SZ. 2004b. Ophiolites from the Mianlue suture in the southern Qinling and their relationship with eastern Paleotethys evolution. *Acta Geologica Sinica*, 78(1): 107–117
- Li SZ, Kusky TM, Wang L, Zhang GW, Lai SC, Liu XC, Dong SW and Zhao GC. 2009. Collision leading to multiple-stage large-scale extrusion: Insights from the Mianlue suture. *Gondwana Research*, 12(1–2): 121–143
- Li ZX, Bogdanova SV, Collins AS, Davidson A, De Waele B, Ernst RE, Fitzsimons ICW, Fuck RA, Gladkochub DP, Jacobs J, Karlstrom KE, Lu S, Natapov LM, Pease V, Pisarevsky SA, Thrane K and Vernikovsky V. 2008. Assembly, configuration, and break-up history of Rodinia: A synthesis. *Precambrian Research*, 160(1–2): 179–210
- Ling WL, Gao S, Cheng JP, Jiang LS, Yuan HL and Hu ZC. 2006. Neoproterozoic magmatic events within the Yangtze continental interior and along its northern margin and their tectonic implication: Constraint from ELA-ICPMS U-Pb geochronology of zircons from the Huangling and Hannan complexes. *Acta Petrologica Sinica*, 22(2): 387–396 (in Chinese with English abstract)
- Liu PJ, Yin CY, Gao LZ, Tang F and Chen SM. 2009. New material of microfossils from the Ediacaran Doushantuo Formation in the Zhangcunping area, Yichang, Hubei Province and its zircon SHRIMP U-Pb age. *Chinese Sci. Bull.*, 54(6): 774–780 (in Chinese)
- Liu SW, Yan QR, Li QG and Wang ZQ. 2009a. Petrogenesis of granitoid rocks in the Kangding Complex, western margin of the Yangtze Craton and its tectonic significance. *Acta Petrologica Sinica*, 25(8): 1883–1896 (in Chinese with English abstract)
- Liu SW, Yang K, Li QG, Wang ZQ and Yan QR. 2009b. Petrogenesis of the Neoproterozoic Baoxing complex and its constraint on the tectonic environment in western margin of Yangtze Craton. *Earth Science Frontiers*, 16(2): 107–118 (in Chinese with English abstract)
- Liu SW, Li QG, Tian W, Wang ZQ, Yang PT, Wang W, Bai X and Guo RR. 2011. Petrogenesis of Indosinian granitoids in middle-segment of South Qinling tectonic belt: Constraints from Sr-Nd isotopic systematics. *Acta Geologica Sinica*, 85(3): 610–628
- Liu SW, Yang PT, Li QG, Wang ZQ, Zhang WY and Wang W. 2011. Indosinian granitoids and orogenic processes in the middle segment of the Qinling Orogen, China. *Journal of Jilin University (Earth Science Edition)*, 41(6): 1928–1943 (in Chinese with English abstract)
- Lu SN, Chen ZH, Li HK, Hao GJ, Zhou HY and Xiang ZQ. 2004. Late Mesoproterozoic-Early Neoproterozoic evolution of the Qinling Orogen. *Geological Bulletin of China*, 23(2): 107–112 (in Chinese with English abstract)
- Mattauer M, Matte PH, Malaveile J, Tapponnier P, Maluslei H, Xu ZQ, Lu YL and Tang YQ. 1985. Tectonics of the Qinling belt: Build-up and evolution of eastern Asia. *Nature*, 317(6037): 496–500
- Meng QR and Zhang GW. 1999. Timing of collision of the North and South China blocks, controversy and reconciliation. *Geology*, 27: 123–126
- Meng QR and Zhang GW. 2000. Geologic framework and tectonic evolution of the Qinling orogen, central China. *Tectonophysics*, 323(3–4): 183–196
- Qin JF, Lai SC and Li YF. 2005. Petrogenesis and geological of Yangba granodiorites from Bikou area, northern margin of Yangtze Plate. *Acta Petrologica Sinica*, 21(3): 697–710 (in Chinese with English abstract)
- Qin JF, Lai SC, Wang J and Li YF. 2007. High-Mg[#] adakitic tonalite from the Xichahe area, South Qinling orogenic belt (central China), petrogenesis and geological implications. *International Geology Review*, 49(12): 1145–1158
- Qin JF, Lai SC and Li YF. 2007. Genesis of the Indosinian guangtoushan adakitic biotite plagiogranite in the Mianxian-Lueyang (Mianlue) suture, South Qinling, China, and its tectonic implications. *Geological Bulletin of China*, 26(4): 466–471 (in Chinese with English abstract)
- Qin JF, Lai SC and Li YF. 2008a. Slab breakoff model for the Triassic post-collisional adakitic granitoids in the Qinling Orogen, central China, zircon U-Pb ages, geochemistry, and Sr-Nd-Pb isotopic constraints. *International Geology Review*, 50(12): 1080–1104
- Qin JF, Lai SC, Wang J and Li YF. 2008b. Zircon LA-ICP MS U-Pb age, Sr-Nd-Pb isotopic compositions and geochemistry of the Triassic post-collisional Wulong adakitic granodiorite in the South Qinling, central China, and its petrogenesis. *Acta Geologica Sinica*, 82(2): 425–437
- Qin JF, Lai SC, Diwu CR, Ju YJ and Li YF. 2010a. Magma mixing origin for the post-collisional adakitic monzogranite of the Triassic Yangba pluton, northwestern margin of the South China block, geochemistry, Sr-Nd isotopic, zircon U-Pb dating and Hf isotopic evidences. *Contributions to Mineralogy and Petrology*, 159(3): 389–409
- Qin JF, Lai SC, Grapes R, Diwu CR, Ju YJ and Li YF. 2010b. Origin of Late Triassic high-Mg adakitic granitoid rocks from the Dongjiangkou area, Qinling orogen, central China, implications for subduction of continental crust. *Lithos*, 120(3–4): 347–367
- Qin JF and Lai SC. 2011. Petrogenesis and Geodynamic Implications of the Late Triassic Granitoids from the Qinling Orogenic Belt. Beijing: Science Press, 1–267 (in Chinese)
- Ratschbacher L, Hacker BR, Calvert A, Webb LE, Grimmer JC, McWilliams MO, Ireland T, Dong SW and Hu J. 2003. Tectonics of the Qinling (Central China), tectonostratigraphy, geochronology, and deformation history. *Tectonophysics*, 366(1–2): 1–53

- Sun WD and Li SG. 1998. Pb isotopes of granitoids suggest Devonian accretion of Yangtze (South China) Craton to North China craton, comment. *Geology*, 26(9): 859–861
- Sun WD, Li SG, Chen YD and Li YJ. 2000. Zircon U-Pb dating of granitoids from South Qinling, Central China and their geological significance. *Geochimica*, 29(3): 209–216 (in Chinese with English abstract)
- Sun WD, Li SG, Chen YD and Li YJ. 2002. Timing of synorogenic granitoids in the South Qinling, central China, constraints on the evolution of the Qinling-Dabie orogenic belt. *Journal of Geology*, 110(4): 457–468
- Wang W, Liu SW, Wu FH, Li QG, Wang ZQ, Yang K, Yan QR, Wang RT and Yang PT. 2011. Emplaced and metallogenetic times of Tongchang diorites, southern Shaanxi Province and its geological implications. *Acta Scientiarum Naturalium Universitatis Pekinensis*, 47(1): 91–102 (in Chinese with English abstract)
- Wang W, Liu SW, Feng YG, Li QG, Wu FH, Wang ZQ, Wang RT and Yang PT. 2012. Chronology, petrogenesis and tectonic setting of the Neoproterozoic Tongchang dioritic pluton at the northwestern margin of the Yangtze Block: Constraints from geochemistry and zircon U-Pb-Hf isotopic systematics. *Gondwana Research*, 22(2): 699–716
- Wang ZQ, Yan QR, Yan Z, Wan T, Jiang CF, Gao LD, Li QG, Chen JL, Zhang YL, Liu P, Xie CL and Xiang ZJ. 2009. New division of the main tectonic units of the Qinling Orogenic Belt, Central China. *Acta Geologica Sinica*, 83(11): 1527–1546 (in Chinese with English abstract)
- Yan Z, Wang ZQ, Yan QR, Wang T, Xiao WJ, Li JL, Han FL, Chen JL and Yang YC. 2006. Devonian sedimentary environments and provenances of the Qinling orogen: Constraints on Late Paleozoic southward accretion of the North China Craton. *International Geology Review*, 48(7): 585–618
- Yan Z, Wang ZQ, Wang T, Yan QR, Xiao WJ, Li JL, Han FL and Chen JL. 2007. Tectonic setting of Devonian sediments in the Qinling orogen: Constraints from detrital modes and geochemistry of clastic rocks. *Acta Petrologica Sinica*, 23(5): 1023–1042 (in Chinese with English abstract)
- Yan Z, Wang ZQ, Yan QR, Wang T and Guo XQ. 2012. Geochemical constraints on the provenance and depositional setting of the Devonian Liuling Group, East Qinling mountains, central China: Implications for the tectonic evolution of the Qinling Orogenic Belt. *Journal of Sedimentary Research*, 82(1): 9–20
- Yang PT, Liu SW, Li QG, Zhang F, Wang ZQ, Wang DS, Wang RT, Yan QR and Yan Z. 2011. Ages of the Laocheng granitoids and crustal growth in the South Qinling tectonic domain, Central China: Zircon U-Pb and Lu-Hf isotopic constrains. *Acta Geologica Sinica*, 85(4): 854–869
- Yang PT, Liu SW, Li QG, Wang ZQ, Wang T and Wang W. 2012. Geochemistry and zircon U-Pb-Hf isotopic systematics of the Ningshan granitoid batholith, middle segment of the South Qinling belt, Central China: Constraints on petrogenesis and geodynamic processes. *Journal of Asian Earth Sciences*, 61: 166–186
- Yang Z, Dong YP, Zhou DW, Yu J and Ma HY. 2008. Geochemistry and geologic significance of basic rocks in the Xiaomoling complex in the Zhashui area, South Qinling, China. *Geological Bulletin of China*, 27(5): 611–617 (in Chinese with English abstract)
- Zhang F, Liu SW, Li QG, Sun YL, Wang ZQ, Yan QR and Yan Z. 2011. Re-Os and U-Pb geochronology of the Erlihe Pb-Zn deposit, Qinling Orogenic Belt, Central China, and constraints on its deposit genesis. *Acta Geologica Sinica*, 85(4): 801–840
- Zhang GW, Meng QR, Yu ZP, Sun Y, Zhou DW and Guo AL. 1996. Orogenesis and dynamics of the Qinling orogen. *Science in China (Series D)*, 39(3): 225–234
- Zhang GW, Zhang BR, Yuan XC and Xiao QH. 2001. Qinling Orogenic Belt and Continent Dynamics. Beijing: Science Press, 1–855 (in Chinese)
- Zhao JH and Zhou MF. 2009. Secular evolution of the Neoproterozoic lithospheric mantle underneath the northern margin of the Yangtze Block, South China. *Lithos*, 107(3–4): 152–168
- Zhao JH, Zhou MF, Zheng JP and Fang SM. 2010. Neoproterozoic crustal growth and reworking of the northwestern Yangtze Block: Constraints from the Xixiang dioritic intrusion, South China. *Lithos*, 120(3–4): 439–452
- Zhao JH, Zhou MF, Yan DP, Zheng JP and Li JW. 2011. Reappraisal of the ages of Neoproterozoic strata in South China: No connection with the Grenvillian orogeny. *Geology*, 39(4): 299–302
- Zhou MF, Yan DP, Kennedy AK, Li YQ and Ding J. 2002. SHRIMP U-Pb zircon geochronological and geochemical evidence for Neoproterozoic arc-magmatism along the western margin of the Yangtze Block, South China. *Earth and Planetary Science Letters*, 196(1–2): 51–57
- Zhou MF, Ma YX, Yan DP, Xia XP, Zhao JH and Sun M. 2006. The Yanbian Terrane (Southern Sichuan Province, SW China): A Neoproterozoic arc assemblage in the western margin of the Yangtze Block. *Precambrian Research*, 144(1–2): 19–38

附中文参考文献

- 陈岳龙, 张本仁, 帕拉提·阿布都卡得尔. 1995. 北秦岭丹凤地区早古生代花岗岩的 Pb、Sr、Nd 同位素地球化学特征. *地质科学*, 30(3): 247–258
- 第五春荣, 孙勇, 袁洪林, 王洪亮, 钟兴平, 柳小明. 2008. 河南登封地区嵩山石英岩碎屑锆石 U-Pb 年代学、Hf 同位素组成及其地质意义. *科学通报*, 53(16): 1923–1934
- 第五春荣, 孙勇, 刘良, 张成立, 王洪亮. 2010. 北秦岭宽坪岩群的解体及新元古代 N-MORB. *岩石学报*, 26(16): 2025–2038
- 杜定汉. 1986. 陕西秦巴地区泥盆系研究. 西安: 西安交通大学出版社, 1–230
- 耿元生, 杨崇辉, 王新社, 杜利林, 任留东, 周喜文. 2008. 扬子地台北缘变质基底演化. 北京: 地质出版社, 1–215
- 凌文黎, 高山, 程建萍, 江麟生, 袁洪林, 胡兆初. 2006. 扬子陆核与陆缘新元古代岩浆事件对比及其构造意义——来自黄陵和汉南侵入杂岩 ELA-ICPMS 锆石 U-Pb 同位素年代学的约束. *岩石学报*, 22(2): 387–396
- 刘鹏举, 尹崇玉, 高林志, 唐烽, 陈寿铭. 2009. 湖北宜昌樟村坪埃迪卡拉系陡山沱组微体化石新材料及锆石 SHRIMP U-Pb 年龄. *科学通报*, 54(6): 774–780
- 刘树文, 闫全人, 李秋根, 王宗起. 2009a. 扬子克拉通西缘康定杂岩中花岗质岩石的成因及其构造意义. *岩石学报*, 25(8): 1883–1896
- 刘树文, 杨凯, 李秋根, 王宗起, 闫全人. 2009b. 新元古代宝兴杂岩的岩石成因及其对扬子西缘构造环境的制约. *地学前缘*, 16(2): 107–118
- 刘树文, 杨朋涛, 李秋根, 王宗起, 张万益, 王伟. 2011. 秦岭中段印支期花岗质岩浆作用与造山过程. *吉林大学学报(地球科学版)*, 41(6): 1928–1943
- 陆松年, 陈志宏, 李怀坤, 郝国杰, 周红英, 相振群. 2004. 秦岭造山带中-新元古代(早期)地质演化. *地质通报*, 23(2): 107–112
- 秦江峰, 赖绍聪, 李永飞. 2005. 扬子板块北缘碧口地区阳坝花岗岩长岩体成因研究及其地质意义. *岩石学报*, 21(3): 679–710
- 秦江峰, 赖绍聪, 李永飞. 2007. 南秦岭勉县-略阳缝合带印支期光头山埃达克质花岗岩的成因及其地质意义. *地质通报*, 26(4): 466–471
- 秦江峰, 赖少聪. 2011. 秦岭造山带晚三叠世花岗岩类成因机制与

- 深部动力学. 北京: 科学出版社, 1-267
- 孙卫东, 李曙光, Chen YD, 李育敬. 2000. 南秦岭花岗岩锆石 U-Pb 定年及其地质意义. 地球化学, 29(3): 209-216
- 王伟, 刘树文, 吴峰辉, 李秋根, 王宗起, 杨凯, 闫全人, 王瑞廷, 杨朋涛. 2011. 陕南铜厂闪长岩体的成岩、成矿时代及其地质意义. 北京大学学报(自然科学版), 47(1): 91-102
- 王宗起, 闫全人, 闫臻, 王涛, 姜春发, 高联达, 李秋根, 陈隽璐, 张英利, 刘平, 谢春林, 向忠金. 2009. 秦岭造山带主要大地构造单元的新划分. 地质学报, 83(11): 1527-1546
- 闫臻, 王宗起, 王涛, 闫全人, 肖文交, 李继亮, 韩芳林, 陈隽璐. 2007. 秦岭造山带泥盆系形成构造环境: 来自碎屑岩组成和地球化学方面的约束. 岩石学报, 23(5): 1023-1042
- 杨钊, 董云鹏, 周鼎武, 于君, 马海勇. 2008. 南秦岭柞水地区小磨岭杂岩基性岩类的地球化学特征及其地质意义. 地质通报, 27(5): 611-617
- 张国伟, 张本仁, 袁学诚, 肖庆辉. 2001. 秦岭造山带与大陆动力学. 北京: 科学出版社, 1-855